Eyes Closed Elevates Brain Intrinsic Activity of Sensory Dominance Networks: A Classifier Discrimination Analysis

Delong Zhang,[1,*] Zhenni Gao,[2,*] Bishan Liang,[3] Junchao Li,[1] Yuxuan Cai,[1] Zengjian Wang,[1] Mengxia Gao,[4] Bingqing Jiao,[1] Ruiwang Huang,[1] and Ming Liu[1]

Abstract

Brain neocortex is usually dominated by visual input (with eyes open [EO]), whereas this visual predominance could be reduced by closing eyes. Cutting off visual input from the eyes (with eyes closed [EC]) would also benefit other sensory performance; however, the neural basis underlying the state-switching remains unclear. In this study, we investigated the brain intrinsic activity of either the EO or EC states by using the resting-state functional magnetic resonance imaging data from 22 healthy participants. The 10 resting-state networks (RSNs) of these participants were explored by the independent component analysis method. Within each RSN, various network parameters (i.e., the amplitude of low-frequency fluctuation, the voxel-wise weighted degree centrality, and the RSN-wise functional connectivity) were measured to depict the brain intrinsic activity properties underlying the EO and EC states. Taking these brain intrinsic activity properties as discriminative features in a linear classifier, we found that the EO and EC states could be effectively classified using the intrinsic properties of the sensory dominance networks and the salience network (SN). Further analysis showed that the brain intrinsic activity within the sensory dominance networks was constantly overwhelmed during the EC state relative to that in the EO state. The SN might play a key role as a switcher between state-switching. Therefore, this study indicated that the brain intrinsic activity in the sensory dominance networks would be enhanced with EC, which might improve other sensory-relative task performance.

Keywords: eyes closed; discriminative analysis; independent component analysis; resting-state functional magnetic resonance imaging; visual dominance

Introduction

THE OPERATION OF BRAIN NEOCORTEX exhibits multisensory properties, in which the visual modality is essentially of predominance (McGurk and MacDonald, 1976). Other sensory-relative task performances could be improved as this visual predominance reduced (Bavelier and Neville, 2002; Colavita, 1974; Merabet et al., 2008; Zubek, 1969). Although the obvious modulation effect of visual modality on brain function has been observed, the underlying neural essence remains unclear.

Brain intrinsic connectivity networks (Seeley et al., 2007) or resting-state networks (RSNs) (Greicius et al., 2003) are highly self-organized brain functional systems and can be characterized in terms of various network properties. Notably, previous studies have shown that the brain activity is response to task performances within a module (Cordes et al., 2000; Greicius et al., 2003). During the resting state, the brain intrinsic activity within or between RSNs has been demonstrated to highly resemble the brain activity during task state (Fox et al., 2006; Mantini et al., 2007; Zuo et al., 2010). Despite this, extensive evidence suggested that the interactions between RSNs exhibit functional implications, which embody the resource integration from different brain intrinsic networks (Bullmore and Sporns, 2012; Cole et al., 2013).

Regarding the brain intrinsic organization, many previous studies have indicated that the intrinsic brain activity properties are affected by the situation whether the subjects have

[1]Center for the Study of Applied Psychology, Key Laboratory of Mental Health and Cognitive Science of Guangdong Province, School of Psychology, South China Normal University, Guangzhou, China.
[2]School of Psychology and Cognitive Science, East China Normal University, Shanghai, China.
[3]Guangdong Polytechnic Normal University, Guangzhou, China.
[4]The State Key Laboratory of Brain and Cognitive Sciences, The University of Hong Kong, Hong Kong, Hong Kong.
*These authors contributed equally to this work.

their eyes open (EO) or eyes closed (EC) (Liang et al., 2014; Yan et al., 2009; Yang et al., 2007). Switching between the EC and EO states could alternate the brain intrinsic activity in many RSNs, such as the visual (Yang et al., 2007), the sensorimotor (Liang et al., 2014; Marx et al., 2004), and the default-mode network (DMN) (Yan et al., 2009; Yang et al., 2007). In addition, previous researches have observed the influences of switching between the EC and EO states on functional connectivity (He et al., 2009; McAvoy et al., 2012; Wu et al., 2010; Yan et al., 2009; Zou et al., 2009) and network topological organization (Jao et al., 2013; Xu et al., 2014). More importantly, the brain intrinsic activity properties could be effectively used to distinguish the EO and EC states (Zhang et al., 2015).

The present study aimed to systematically investigate the modulation effect between the EC and EO states on an aspect of the brain RSNs by using a linear classifier discrimination approach. To this end, we collected the resting-state functional magnetic resonance imaging (rs-fMRI) data from 22 healthy participants under the EO and EC states, and we adopted the independent component analysis (ICA) to identify in total of 10 RSNs. Then, the intrinsic activity properties, that is, the amplitude of low-frequency fluctuation (ALFF), the voxel-wise weighted degree centrality (WDC), and the functional connectivity strength (FCS) of each RSN were measured. These RSN properties were used as classification features in a linear classifier discrimination analysis to distinguish the EC and EO states and to determine the contributions of each RSN on discrimination.

Materials and Methods

Participants

We recruited 22 right-handed healthy voluntaries (11 males/11 females, 20 ± 2.74 years) from the Beijing Normal University for the present study. This study was approved by the institutional review board of the Beijing Normal University Imaging Center for Brain Research. Written informed consent was given by each participant. All the participants were paid as compensation for their participation. Participants were instructed about the two conditions (i.e., EO and EC) before the fMRI scanning. To prevent the participants from falling into sleep while scanning, participants were instructed to perform a ''pseudo'' arithmetic judgment task in which the arithmetic question presented in an auditory form. Participants would press the left button when the question was correct, otherwise, would press the right button. This procedure was designed to make sure that these participants stayed awake during the EO and EC states. However, there were actually no tests during the real scanning procedure so as to retain the purity of the resting-state data.

Data acquisition

All participants were scanned on a 3T Siemens Trio TIM MR scanner equipped with a 12-channel, phased array receiver-only head coil at the Imaging Center for Brain Research, Beijing Normal University, using a gradient-echo echo planar imaging (EPI) sequence with the following parameters: TR = 2000 ms, TE = 30 ms, 33 transverse slices, slice thickness = 3.5 mm, gap = 0.7 mm, flip angle = 90°, FOV = 224 × 224 mm, matrix = 64 × 64, and 240 volumes covering the whole brain. The rs-fMRI scans of the EC (lasting for 8 min) and EO (lasting for 8 min) conditions from each participant were obtained in the same session. The acquisition order of the EC and EO scan data were counterbalanced across all participants. In addition, this study also collected a high-resolution 3D brain structural image for each participant using the MP-RAGE sequence with the implementation of the parallel imaging scheme GeneRalized Autocalibrating Partially Parallel Acquisitions (GRAPPA) (Griswold et al., 2002) and an acceleration factor of 2.

Data preprocessing

Data preprocessing was performed using the GRETNA toolbox (Wang et al., 2015) and SPM8 (www.fil.ion.ucl.ac.uk/spm). The first four functional images were discarded because of the initial scanning signal instability. The remaining functional images were corrected for within-scan acquisition time differences between slices, and then, all images were realigned to the first volume due to head motion. The excessive head motion of all the subject image data met the criteria of >1 mm displacement or an angular rotation of >1° in any direction. The summary scalars of both gross (maximum and root mean square) and micro (mean framewise displacement) head motion were matched between the two states (all $p > 0.14$). Using an optimum 12-parameter affine transformation and nonlinear deformations, the motion-corrected data were then spatially normalized onto the Montreal Neurological Institute space and resampled to a voxel size of $3 \times 3 \times 3 \text{ mm}^3$. Subsequently, low-frequency temporal band-pass filtering (0.01–0.1 Hz) was performed on the time series of each voxel. Besides removing the linear trend, several nuisance signals, including 24-parameter head-motion profiles (Friston et al., 1996; Yan et al., 2013), mean white matter signals, and cerebrospinal fluid signals, were also regressed out from each voxel's time course. Notably, unless otherwise stated, no spatial smoothing was applied in the data processing as previous studies have found that smoothing could induce spurious local correlations (Zuo et al., 2012).

Spatial ICA

We used GIFT (http://icatb.sourceforge.net) to perform the spatial ICA to identify brain intrinsic networks under the EO and EC states. First, the spatial smoothing with a Gaussian kernel of 8 mm full-width at half-maximum was conducted to the preprocessed rs-fMRI data. Second, we performed the principle component analysis (PCA) to reduce the data dimensions. Herein, we calculated PCA in two steps: the data for each individual participant were temporally dimension-reduced, and then, the dimensions were again reduced to the optimal numbers after concatenation across subjects within groups. Third, the data were separated by ICA using an extended infomax algorithm (Lee et al., 1999). After ICA separation, the mean independent components and the corresponding mean time courses over all the participants were used for the back-reconstruction of the independent components and the time courses for each individual participant (Calhoun et al., 2001). Finally, the intensity values in each independent component spatial map were converted to Z-scores, and a one sample t-test (false discovery rate [FDR],

$p = 0.01$) was then performed under the EO and EC states to determine the RSNs.

Brain intrinsic activity metrics

Amplitude of low-frequency fluctuation. The ALFF (Yang et al., 2007) is applied to measure the spontaneous neural activity within each voxel of the whole brain by using the preprocessed data. ALFF is defined as the total power within the frequency range between 0.01 and 0.1 Hz and thus indexes the strength or intensity of low-frequency oscillations (Yu-Feng et al., 2007).

In this study, the ALFF calculation was carried out using GRETNA. The preprocessed time series of each voxel was first transformed to the frequency domains by using fast Fourier transform. Then, the square root was calculated at each frequency of the power spectrum, and the averaged square root was obtained across 0.01–0.1 Hz, which was taken as the ALFF. Finally, the ALFF of each voxel was divided by the global mean ALFF value in each participant for normalization.

Voxel-wise WDC. The voxel-wise WDC based on graph theory was used to quantify the functional integration of each voxel with others in a network. Degree centrality (DC) is the number of edges connecting to a node. For a weighted graph, it is defined as the sum of weights from edges connecting to a node or the node strength. DC can be computed as the formula:

$$DC(i) = \sum_{j=1}^{N} \alpha_{ij}.$$

All nodes are defined $1 \le i \le N$, $1 \le j \le N$, and α_{ij} represents the connection or edge from node i to node j.

The functional integration was measured using the FCS indicated by the Pearson correlation coefficients of the BOLD (blood oxygen level-dependent) signals between each specific voxel and the rest of other voxels. All the selected voxels were masked by the grey matter probability map in SPM8 (threshold = 0.2). A threshold procedure was used to remove the spurious weak correlations, in which the statistical significance was set at the level of $p < 0.05$ (Bonferroni corrected). Particularly, only the positive correlation was included into the calculation because of the ambiguous interpretation and detrimental effects of the negative correlation on test–retest reliability (Fox et al., 2009; Murphy et al., 2009; Wang et al., 2011; Weissenbacher et al., 2009). And a distance threshold was set at 75 mm to classify the long and short functional connectivity (He et al., 2009); thus, there were three types of WDC (i.e., long-degree-centrality [LDC], short-degree-centrality [SDC], and DC) acquired for each participant. Based on these metrics, the values of the DC at each voxel indicated the different functional integrations over the whole brain. Of note, the WDC was normalized within each individual by translating to Z-scores using the GRETNA toolbox.

RSN-wise FCS. The mean time series of each RSN were extracted to calculate the inter- and intra-RSN FCS. Pearson correlation coefficients between the mean time series of any possible pair of the 10 RSNs were calculated, which led to a 10×10 correlation matrix for each subject. Finally, the average correlation of each RSN with other RSNs was measured using a previous method (He et al., 2009; Jiang et al., 2004). In this method, the FCS between two RSNs was equally divided into the two RSNs.

Discriminative analyses

A maximum uncertainty linear discriminant analysis (MLDA) (Thomaz et al., 2004, 2007) was used to classify the EC and EO states. A previous study suggested that the MLDA approach seeks a set of projection directions that maximize the between-class margin and simultaneously minimize the within-class compactness (Dai et al., 2014). Based on this classifier, the EC and EO label can be mapped onto the discrimination hyperplane, and the amount of discriminative feature can be quantified using the coefficients of the discrimination hyperplane. A leave-one-out cross-validation approach was adopted to optimize the feature selection by reducing the data dimensions ($p < 0.05$, paired two-tailed t-tests, FDR correction). The feature selection was performed only in the training data so as to keep the independence of the training data and the test data. By using a linear classifier, the contribution of the single RSN property (e.g., WDC) to discrimination was evaluated, independently. After classification, we explored whether the classification accuracy was significantly above the random level by using an approach, which randomly disturbed the order of category labels to repeat the classification process ($n = 100$).

Besides the single linear classifier approach, a multi-classifier approach (each RSN property corresponding to a linear classifier) was applied to investigate the concatenate effect of all these RSN properties (i.e., ALFF, LDC, SDC, DC, and FSC) on the classification performance. In this multi-classifier discrimination process, a weighted voting method was used to evaluate the contribution of these RSN properties to classification. Notably, using this approach, the weight of each RSN property on classification was first evaluated with each single linear classifier (one RSN property related to a linear classifier), and then, the weight of these RSN properties from different classifiers was further calculated by using a voting approach (for details, see Dai et al., 2012). And finally, the significance of the multi-classifier discrimination results was evaluated using the approach as the single linear classifier.

To date, the multi-classifier method has been successfully used to identify Alzheimer's disease (AD) patients from normal controls (Dai et al., 2012) and to distinguish the resting-state and task-state fMRI (Gao et al., 2017). The more detailed information of this method could also be found in these previous studies (Dai et al., 2012; Gao et al., 2017).

Results

Resting-state networks

We identified 10 brain functional RSNs by using the spatial ICA method. These RSNs include the anterior DMN, the auditory network, the central executive network, the dorsal attention network, the high-level visual network (HVN), the posterior DMN, the primary sensory-motor network (PSMN), the primary visual network (PVN), the salience network (SN), and the ventral motor network (VMN) (Fig. 1 and Table 1).
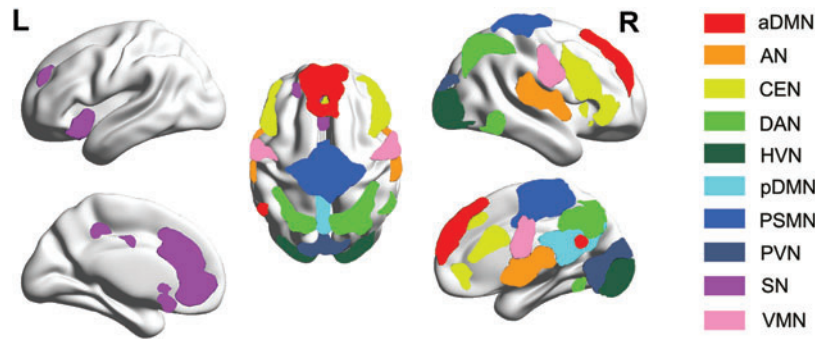
FIG. 1. RSNs derived from the spatial ICA analysis. aDMN, anterior default-mode network; AN, auditory network; CEN, central executive network; DAN, dorsal attention network; HVN, high-level visual network; ICA, independent component analysis; pDMN, posterior default-mode network; PSMN, primary sensory-motor network; PVN, primary visual network; RSNs, resting-state networks; SN, salience network; VMN, ventral motor network. Color images are available online.

Brain intrinsic activity metrics

We also calculated the voxel-wise ALFF, LDC, SDC, and DC metrics and RSN-wise FCS metric of these 10 brain RSNs for each participant under the EC and EO states, separately (Fig. 2).

Univariate comparisons of RSN intrinsic activity

By using a paired two-tailed t-test, we statistically compared all the brain intrinsic activity properties of each RSN we measured between the EO and EC states. The results showed that the ALFF under the EC state was significantly higher than that in the EO state in the PSMN ($p = 0.0061$, FDR) and the VMN ($p = 0.0062$, FDR). Higher LDC in the EC state than in the EO state was observed to be statistically significant in the PVN ($p = 0.0001$, FDR), the HVN ($p = 0.0004$, FDR), the PSMN ($p = 0.0005$, FDR), and the VMN ($p = 0.0039$, FDR). However, the EO state exhibited a higher LDC than the EC state in the SN ($p = 0.0029$, FDR). The SDC of the PSMN ($p = 0.0006$, FDR) in the EC

state was higher than that in the EO state. The EC state obtained a higher DC in the HVN ($p = 0.0077$, FDR), the PSMN ($p = 0.0002$, FDR), and the VMN ($p = 0.0213$, FDR), but a lower DC in the SN compared with the EO state. On an aspect of FCS, the EC state exhibited a higher functional connectivity integration in the PVN ($p = 0.0026$, FDR) and the HVN ($p = 0.0061$, FDR) than the EO state (Table 2).

Discrimination performance

By using MLDA, this study found that the selected RSN properties exhibited a discriminative power to distinguish the EC and EO states (Table 3). The discriminative accuracy of the classifier with each of the RSN properties (i.e., ALFF, LDC, SDC, DC, and FCS) as features was significantly above the random level (all $p < 0.05$), respectively. More importantly, by using a multi-classifier approach, the present findings showed that the concatenate effect of these RSN properties could obviously improve the classification accuracy (Table 3).

TABLE 1. DETAILS OF THE SELECTED RESTING-STATE NETWORKS

Index	RSNs	Regions	Coordinates			t
			X	Y	Z	
1	aDMN	Frontal_Sup_Medial_L	0	54	15	18.59
2	AN	Temporal_Sup_L	−54	−12	6	18.59
3	CEN	Frontal_Inf_Tri_R	51	27	27	14.33
4	DAN	Parietal_Sup_L	−18	−75	51	19.68
5	HVN	Occipital_Sup_R	24	−102	9	19.24
6	pDMN	Cingulum_Mid_R	3	−30	30	25.31
7	PSMN	Supp_Motor_Area_R	3	−15	69	17.98
8	PVN	Lingual_R	6	−84	−3	18.75
9	SN	Cingulum_Ant_L	−9	39	−3	24.27
10	VMN	Postcentral_R	60	−6	33	18.88

The coordinates are the peak voxel value of each RSN in MNI space. The regions are those in which the peak voxels were located at. The *t*-value indicates the scores of the one-sample *t*-test ($p < 0.001$, FDR corrected).

aDMN, anterior default-mode network; AN, auditory network; CEN, central executive network; DAN, dorsal attention network; FDR, false discovery rate; HVN, high-level visual network; L, left hemisphere; MNI, Montreal Neurological Institute; pDMN, posterior default-mode network; PSMN, primary sensory-motor network; PVN, primary visual network; R, right hemisphere; RSN, resting-state network; SN, salience network; VMN, ventral motor network.
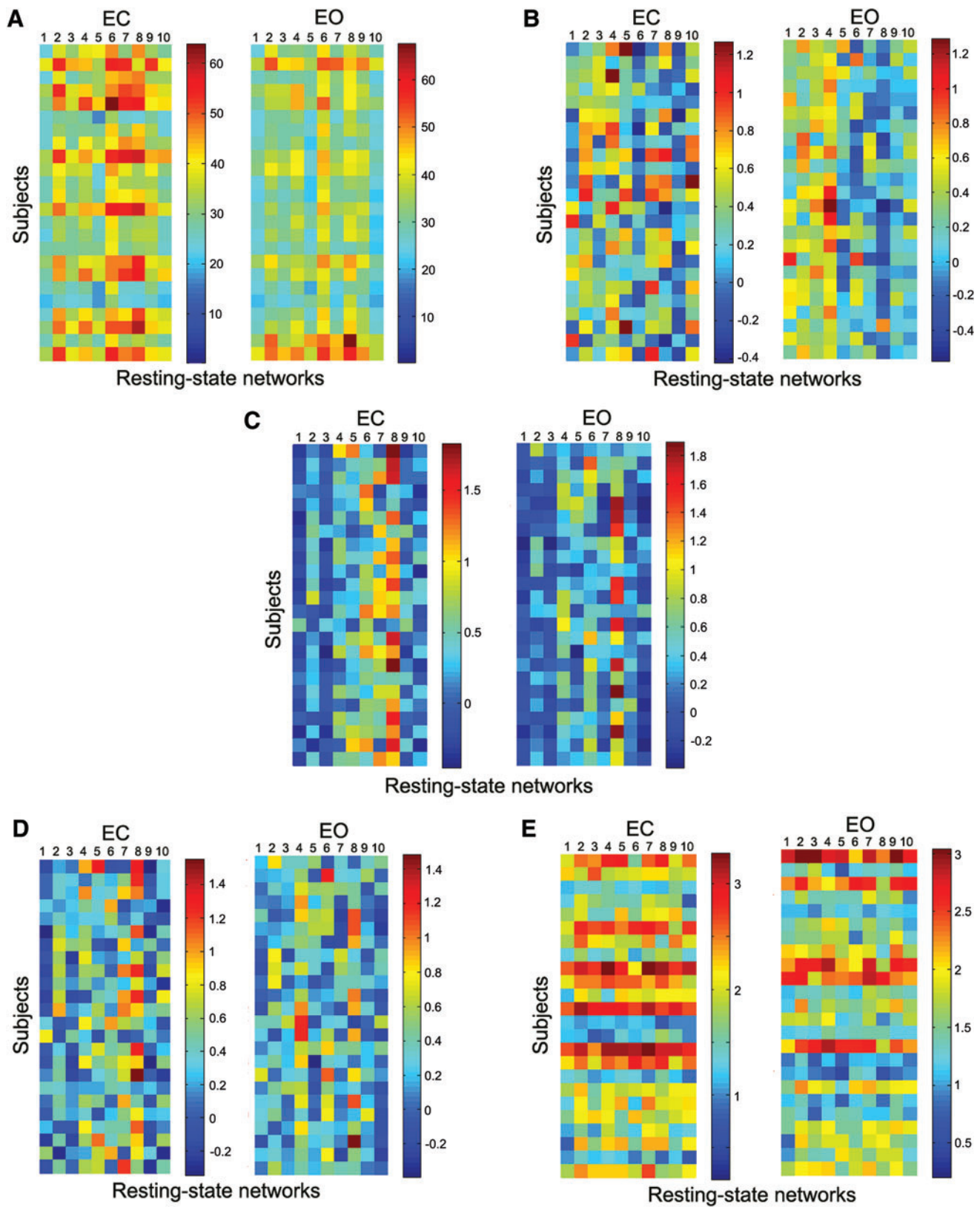
FIG. 2. The maps of ALFF, LDC, SDC, DC, and FCS across 10 RSNs of EC and EO. **(A)** ALFF; **(B)** LDC; **(C)** SDC; **(D)** DC; **(E)** FCS. One to 10 represent aDMN, AN, CEN, DAN, HVN, pDMN, PSMN, PVN, SN, and VMN. These RSNs were selected using a one sample *t*-test (FDR, $p = 0.01$). ALFF, amplitude of low-frequency fluctuation; DC, degree centrality; EC, eyes closed; EO, eyes open; FCS, functional connectivity strength; FDR, false discovery rate; LDC, long-degree-centrality; SDC, short-degree-centrality. Color images are available online.

TABLE 2. RESULTS OF COMPARISONS OF RESTING-STATE NETWORK INTRINSIC ACTIVITY
BETWEEN EYES CLOSED AND EYES OPEN

	aDMN	AN	CEN	DAN	HVN	pDMN	PSMN	PVN	SN	VMN
ALFF										
p	0.907	0.099	0.960	0.788	0.348	0.428	0.006	0.538	0.748	0.006
t-stat	−0.118	1.682	−0.051	0.271	0.949	0.799	2.877**	0.620	0.324	2.871**
Delta	−0.160	3.919	−0.075	0.537	1.920	1.548	7.675	1.865	0.538	5.199
LDC										
p	0.1964	0.4855	0.0876	0.2573	0.0004	0.0704	0.0005	0.0001	0.0029	0.0039
t-stat	−1.3109	0.7032	−1.7455	−1.1469	3.8406**	−1.8523	3.7353**	4.3699**	−3.1521**	3.0354**
Delta	−0.1050	0.0542	−0.1064	−0.0913	0.3447	−0.1678	0.3077	0.4531	−0.1624	0.2579
SDC										
p	0.2784	0.3389	0.1883	0.1757	0.1507	0.4359	0.0006	0.6322	0.1952	0.1314
t-stat	−1.0969	0.9665	−1.3355	−1.3752	1.4613	0.7861	3.6726**	0.4818	−1.3145	1.5359
Delta	−0.0587	0.0761	−0.0688	−0.1165	0.1363	0.0730	0.4007	0.0705	−0.0944	0.1280
DC										
p	0.2367	0.3801	0.1561	0.1458	0.0077	0.5815	0.0002	0.0498*	0.0412	0.0213
t-stat	−1.1988	0.8863	−1.4421	−1.4797	2.7897**	−0.5551	4.0751**	20.148*	−2.1000*	2.3837*
Delta	−0.0837	0.0735	−0.0851	−0.1233	0.2472	−0.0542	0.3955	0.2437	−0.1368	0.2120
FCS										
p	0.3418	0.0833	0.1781	0.1805	0.0061	0.1684	0.0611	0.0026	0.4888	0.0983
t-stat	0.9605	1.7704	1.3677	1.3600	2.8724**	1.3993	1.9195	3.1782**	0.6978	1.6872
Delta	0.1509	0.2914	0.2414	0.2444	0.5011	0.2273	0.3361	0.5172	0.1099	0.3062

Delta value = EC − EO.
*$p < 0.05$; **$p < 0.01$.
ALFF, amplitude of low-frequency fluctuation; DC, degree centrality; EC, eyes closed; EO, eyes open; FCS, functional connectivity strength; LDC, long-degree-centrality; SDC, short-degree-centrality.

Contribution of RSNs in discrimination

By using these RSN properties as classification features, the present study used the MLDA classifier to discriminate the EO and EC states. All the selected features and their relative weights in each classifier are shown in Figure 3. We found that the well-identified features are mainly located at the visual network, the sensorimotor-related network, and the SN. It should be noted that the spontaneous activity amplitude (ALFF) and the functional connectivity strength (DC, LDC, SDC, and FCS) contributed differently in the classification performance. On an aspect of ALFF, we found that the sensorimotor-related networks (i.e., the PSMN and the VMN) took important roles in classification of the two states. As to the FCS, the visual network and the SN as well as the sensorimotor network were essential as features to discriminating the two states. Furthermore, the different types of RSN properties performed differently on discrimination. For details, the short-term functional connectivity (SDC) of the PSMN could effectively discriminate the two states, but the visual network, the sensorimotor network, and the SN were more sensitive to long-term functional connectivity (LDC) for the classification. In addition, the voxel-wise functional connectivity and the RSN-wise functional connectivity carried discriminative information in classification of the EO and EC states. The visual network performed well on the RSN-wise functional connectivity, whereas the visual network and the sensorimotor network achieved classification performance from the voxel-wise functional connectivity features.

Discussion

By using MLDA, our study explored the alternation of the brain intrinsic activity between the EC and EO states. The main findings can be summarized as follows: (i) the intrinsic activity of sensory dominance networks (i.e., sensorimotor and visual networks) was significantly modulated by switching between the EC and EO states; (ii) the SN may play an important role when the spontaneous amplitude activity and the functional integration of sensory dominance networks were altered between the EC and EO states; (iii) the brain intrinsic activity in the sensory dominance networks enhanced during the EC state compared with the EO state.

Previous studies have documented that there are distinct mental states between the EO and EC states (Marx et al., 2003; Mazard et al., 2005). There is an ''exteroceptive'' mental activity state that includes the ocular motor and attention

TABLE 3. THE CLASSIFIER PERFORMANCE IN DISCRIMINATING THE EYES CLOSED AND EYES OPEN CONDITIONS

	ALFF	LDC	SDC	DC	FCS	Concatenate features
Sensitivity	0.8333	0.9167	0.6250	0.7083	0.7917	0.8750
Specificity	0.5833	0.6250	0.7083	0.6250	0.7083	0.7500
Accuracy	0.7083*	0.7708*	0.6667*	0.6667*	0.7500*	0.8125*

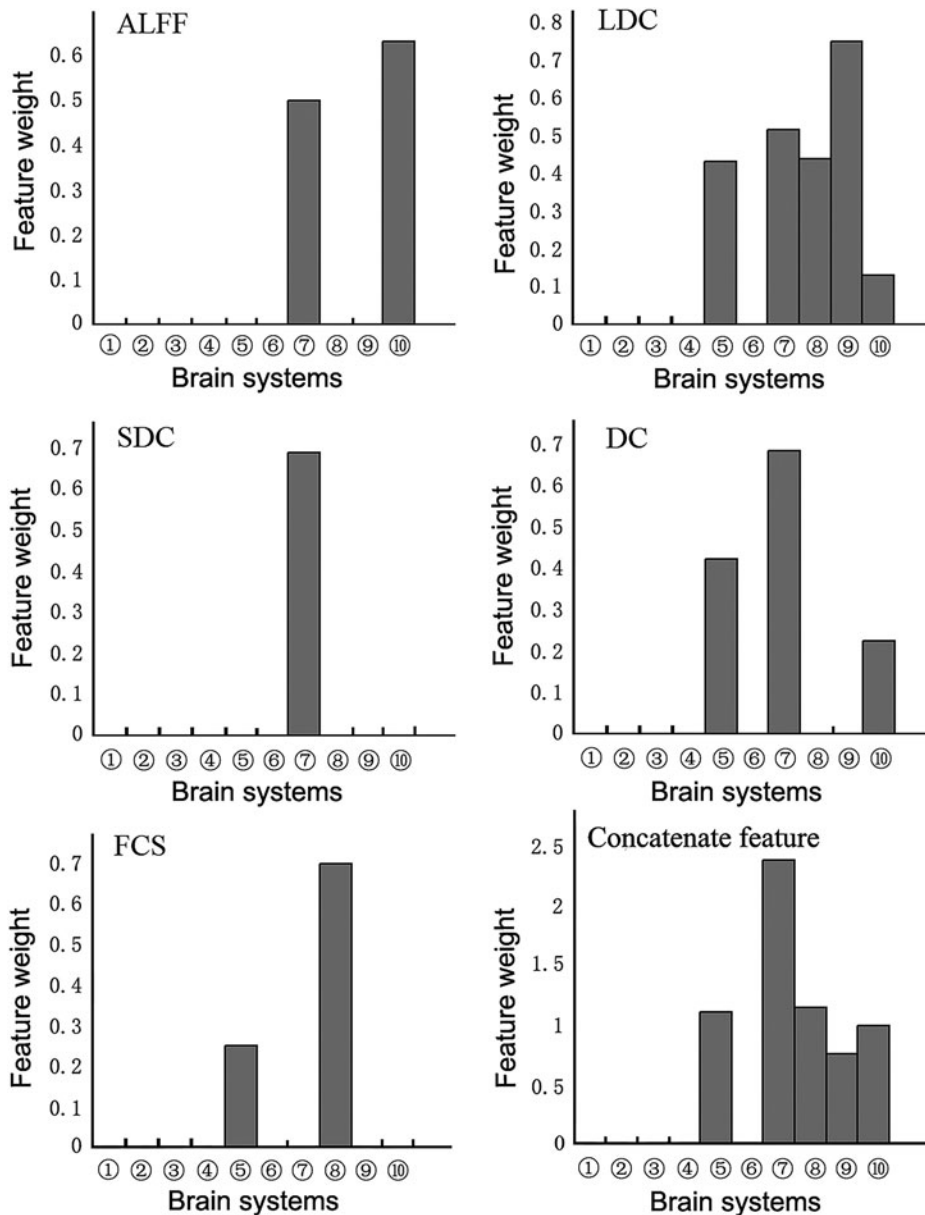Concatenate feature, all the above features used for classification, *$p < 0.05$.

FIG. 3. The features for classification with discriminative power related to 10 RSNs.

① aDMN; ② AN; ③ CEN; ④ DAN; ⑤ HVN;
⑥ pDMN; ⑦ PSMN; ⑧ PVN; ⑨ SN; ⑩ VMN.

activity during EO, and an ''interoceptive'' mental activity state of multisensory and imagination activity during EC (Marx et al., 2003, 2004). Previous electroencephalography (EEG) studies also indicated that the distinct oscillatory signatures have been identified in the alpha-band at prestimulus that relates to an upcoming visual stimulus process (Fox and Raichle, 2007; Foxe and Snyder, 2011). Similarly, these findings suggested that the alpha-band power increased on the EC states (Fox and Raichle, 2007). In other words, it suggested that the neural spontaneous fluctuation activity constitutes a visual operation mode that is activated automatically even without retinal input.

It should be noted that the exteroceptive and interoceptive states may be related to specific brain activity patterns (Marx et al., 2003, 2004). Correspondingly, many previous studies

have provided experimental evidence that the eye behavioral states (e.g., the EO and EC states) modulate the brain spontaneous fluctuation activity within several systems, including the sensorimotor network (Assaf et al., 2006; Mazard et al., 2002, 2005), the visual network (Yang et al., 2007), and the DMN (Yan et al., 2009). Our previous study, using the support vector machine, found that the spontaneous fluctuation activity of the sensorimotor network could directly classify the EO and EC states (Zhang et al., 2015). Furthermore, the present study also showed that the fluctuation amplitude pattern related to the sensorimotor and visual networks could accurately distinguish the EC and EO states. The well-identified features for the classification were primarily derived from the intrinsic properties in the primary visual cortex, the high visual cortex, the VMN, and the PSMN.

Beyond this, we also found that the functional interaction properties of the sensory-motor network (SMN) and the visual network (VSN) performed well in the classification of the two states. In particular, our study showed that the voxel-wise and the RSN-wise FCS contributed differently to the classification. On the RSN-wise FCS, we found that the visual network (i.e., PVN and HVN) took important role in the classification. While, on the voxel-wise FCS, the HVN and the sensorimotor network (PSMN and VMN) exhibited great power in classification. More importantly, we also found that the different types of voxel-wise FCS performed differently. On the short-term voxel-wise FCS, we found that the PSMN is a core network to classify the two states; but on an aspect of the long-term FCS, we found that the visual network (PVN and HVN), the sensorimotor network (PSMN and VMN), and the SN converged to show great power in the classification. Of note, we observed that the spontaneous activity of sensorimotor network was associated with that of the PVN when participants stayed in the EC state (Wang et al., 2008). This observation may show that the mental imagery-related pattern is an important aspect of the difference of the EC and EO states. Moreover, the SN may take an important role in this process. Previous studies have demonstrated that the SN plays a role that may reflect dynamic switching between large-scale networks (Beaty et al., 2015; Seeley et al., 2007). Similarly, a previous study of our group showed that the functional connectivity directionality of the SN within a Bayesian network could effectively discriminate the two states (Zhang et al., 2015). In this study, we also found that the concatenate effect of the salience, sensorimotor, and visual networks in classification. Potentially, the mental imagery-related neural activity underlying the modulation of the SN is a characteristic of the change between the EC and EO states. Nevertheless, these findings will help to understand the neural substrate of brain functional reconfiguration underlying the switch between the EC and EO states.

Although the involved regions were distinct in terms of different types of features, all these observed features were predominately located at the SMN and VSN and were consistently improved in the EC state compared with the EO state. It should be noted that the visual deprivation may improve performance of other-modal perception, and even the immediate visual deprivation (e.g., eye closure) can enhance somatosensory processing sensitivity (Stronks et al., 2015). Corresponding to these observations, this study also figured out the improvement of the intrinsic activity of sensorimotor network in terms of the ALFF and FCS. Besides this, our study found that the intrinsic activity of the VSN was also improved during the EC state when compared with that of the EO state. These findings were highly corresponding to many previous studies which found that the BOLD signal variability was significantly improved during the EC state when compared with that of the EO state (Bianciardi et al., 2009; Fukunaga et al., 2006; Horovitz et al., 2008; Jao et al., 2013; Liang et al., 2014). An important issue should attracted attention is that the level of glucose metabolism in visual regions was significantly decreased during the EC state (Riedl et al., 2014) as well as the change of regional cerebral blood flow (Zou et al., 2015). That is, there is a low level of energy metabolism during the EC state related to the EO state; the physiological findings may provide new evidence to support the Chinese old sayings that "to conserve energies by closing the eyes." Despite this, the intrinsic activity measured by the BOLD signal was significantly improved not only in the visual networks but also in other sensory dominance networks such as the sensorimotor network, and the higher intrinsic activity may be corresponding to a specific mental state in which the imagination process is of importance, which may be related to the vividness imagery occurring in the resting mind especially during the EC state.

Conclusion

This study employed a linear classifier discriminative approach to identify the brain intrinsic activity in classification of the EC and EO states. We found that the spontaneous amplitude activity and the functional integration properties of the sensory dominance networks (i.e., sensorimotor and visual networks) and the SN were significantly stronger during the EC state compared with the EO state. The results support the proposition that the EC state may induce a specific mental state with enhanced intrinsic activity of sensory dominance networks underlying the modulation of the SN. Our findings might help understand the neural substrate of the brain functional reconfiguration that underlies the alternation between distinct mental states (i.e., the EC and EO states).

Acknowledgment

Author Disclosure Statement

No competing financial interests exist.

References

Assaf M, Calhoun VD, Kuzu CH, Kraut MA, Rivkin PR, Hart J, et al. 2006. Neural correlates of the object-recall process in semantic memory. Psychiatry Res 147:115–126.

Bavelier D, Neville HJ. 2002. Cross-modal plasticity: where and how? Nat Rev Neurosci 3:443–452.

Bianciardi M, Fukunaga M, van Gelderen P, Horovitz SG, de Zwart JA, Duyn JH. 2009. Modulation of spontaneous fMRI activity in human visual cortex by behavioral state. Neuroimage 45:160–168.

Bullmore E, Sporns O. 2012. The economy of brain network organization. Nat Rev Neurosci 13:336–349.

Calhoun VD, Adali T, Pearlson GD, Pekar J. 2001. A method for making group inferences from functional MRI data using independent component analysis. Hum Brain Mapp 14:140–151.

Colavita FB. 1974. Human sensory dominance. Percept Psychophys 16:409–412.

Cole MW, Reynolds JR, Power JD, Repovs G, Anticevic A, Braver TS. 2013. Multi-task connectivity reveals flexible hubs for adaptive task control. Nat Neurosci 16:1348–1355.

Cordes D, Haughton VM, Arfanakis K, Wendt GJ, Turski PA, Moritz CH, et al. 2000. Mapping functionally related regions of brain with functional connectivity MR imaging. Am J Neuroradiol 21:1636–1644.

Dai Q, Sun DW, Xiong Z, Cheng JH, Zeng XA. 2014. Recent advances in data mining techniques and their applications in hyperspectral image processing for the food industry. Compr Rev Food Sci Food Saf 13:891–905.

Dai Z, Yan C, Wang Z, Wang J, Xia M, Li K, et al. 2012. Discriminative analysis of early Alzheimer's disease using multi-modal imaging and multi-level characterization with multi-classifier (M3). Neuroimage 59:2187–2195.

Fox MD, Raichle ME. 2007. Spontaneous fluctuations in brain activity observed with functional magnetic resonance imaging. Nat Rev Neurosci 8:700–711.

Fox MD, Snyder AZ, Zacks JM, Raichle ME. 2006. Coherent spontaneous activity accounts for trial-to-trial variability in human evoked brain responses. Nat Neurosci 9:23–25.

Fox MD, Zhang D, Snyder AZ, Raichle ME. 2009. The global signal and observed anticorrelated resting state brain networks. J Neurophysiol 101:3270–3283.

Foxe JJ, Snyder AC. 2011. The role of alpha-band brain oscillations as a sensory suppression mechanism during selective attention. Front Psychol 2:154.

Friston KJ, Williams S, Howard R, Frackowiak RSJ, Turner R. 1996. Movement-related effects in fMRI time-series. Magn Reson Med 35:346–355.

Fukunaga M, Horovitz SG, van Gelderen P, de Zwart JA, Jansma JM, Ikonomidou VN, et al. 2006. Large-amplitude, spatially correlated fluctuations in BOLD fMRI signals during extended rest and early sleep stages. Magn Reson Imaging 24:979–992.

Gao M, Zhang D, Wang Z, Liang B, Cai Y, Gao Z, et al. 2017. Mental rotation task specifically modulates functional connectivity strength of intrinsic brain activity in low frequency domains: a maximum uncertainty linear discriminant analysis. Behav Brain Res 320:233–243.

Greicius MD, Krasnow B, Reiss AL, Menon V. 2003. Functional connectivity in the resting brain: a network analysis of the default mode hypothesis. Proc Natl Acad Sci U S A 100:253–258.

Griswold MA, Jakob PM, Heidemann RM, Nittka M, Jellus V, Wang J, et al. 2002. Generalized autocalibrating partially parallel acquisitions (GRAPPA). Magn Reson Med 47:1202–1210.

He Y, Dagher A, Chen Z, Charil A, Zijdenbos A, Worsley K, et al. 2009. Impaired small-world efficiency in structural cortical networks in multiple sclerosis associated with white matter lesion load. Brain 132:3366–3379.

Horovitz SG, Fukunaga M, de Zwart JA, van Gelderen P, Fulton SC, Balkin TJ, et al. 2008. Low frequency BOLD fluctuations during resting wakefulness and light sleep: a simultaneous EEG-fMRI study. Hum Brain Mapp 29:671–682.

Jao T, Vértes PE, Alexander-Bloch AF, Tang I-N, Yu Y-C, Chen J-H, et al. 2013. Volitional eyes opening perturbs brain dynamics and functional connectivity regardless of light input. Neuroimage 69:21–34.

Jiang T, He Y, Zang Y, Weng X. 2004. Modulation of functional connectivity during the resting state and the motor task. Hum Brain Mapp 22:63–71.

Lee T-W, Girolami M, Sejnowski TJ. 1999. Independent component analysis using an extended infomax algorithm for mixed subgaussian and supergaussian sources. Neural Comput 11:417–441.

Liang B, Zhang D, Wen X, Xu P, Peng X, Huang X, et al. 2014. Brain spontaneous fluctuations in sensorimotor regions were directly related to eyes open and eyes closed: evidences from a machine learning approach. Front Hum Neurosci 8:645.

Mantini D, Perrucci MG, Del Gratta C, Romani GL, Corbetta M. 2007. Electrophysiological signatures of resting state networks in the human brain. Proc Natl Acad Sci U S A 104:13170–13175.

Marx E, Deutschländer A, Stephan T, Dieterich M, Wiesmann M, Brandt T. 2004. Eyes open and eyes closed as rest conditions: impact on brain activation patterns. Neuroimage 21:1818–1824.

Marx E, Stephan T, Nolte A, Deutschländer A, Seelos KC, Dieterich M, et al. 2003. Eye closure in darkness animates sensory systems. Neuroimage 19:924–934.

Mazard A, Laou L, Joliot M, Mellet E. 2005. Neural impact of the semantic content of visual mental images and visual percepts. Brain Res Cogn Brain Res 24:423–435.

Mazard A, Mazoyer B, Etard O, Tzourio-Mazoyer N, Kosslyn SM, Mellet E. 2002. Impact of fMRI acoustic noise on the functional anatomy of visual mental imagery. J Cogn Neurosci 14:172–186.

McAvoy M, Larson-Prior L, Ludwikow M, Zhang D, Snyder AZ, Gusnard DL, et al. 2012. Dissociated mean and functional connectivity BOLD signals in visual cortex during eyes closed and fixation. J Neurophysiol 108:2363–2372.

McGurk H, MacDonald J. 1976. Hearing lips and seeing voices. Nature 264:746.

Merabet LB, Hamilton R, Schlaug G, Swisher JD, Kiriakopoulos ET, Pitskel NB, et al. 2008. Rapid and reversible recruitment of early visual cortex for touch. PLoS One 3:e3046.

Murphy K, Birn RM, Handwerker DA, Jones TB, Bandettini PA. 2009. The impact of global signal regression on resting state correlations: are anti-correlated networks introduced? Neuroimage 44:893–905.

Riedl V, Bienkowska K, Strobel C, Tahmasian M, Grimmer T, Förster S, et al. 2014. Local activity determines functional connectivity in the resting human brain: a simultaneous FDG-PET/fMRI study. J Neurosci 34:6260–6266.

Seeley WW, Menon V, Schatzberg AF, Keller J, Glover GH, Kenna H, et al. 2007. Dissociable intrinsic connectivity networks for salience processing and executive control. J Neurosci 27:2349–2356.

Stronks HC, Nau AC, Ibbotson MR, Barnes N. 2015. The role of visual deprivation and experience on the performance of sensory substitution devices. Brain Res 1624:140–152.

Thomaz CE, Boardman JP, Hill DL, Hajnal JV, Edwards DD, Rutherford MA, et al. Using a maximum uncertainty LDA-based approach to classify and analyse MR brain images. In International Conference on Medical Image Computing and Computer-Assisted Intervention. Berlin: Springer, 2004, pp. 291–300.

Thomaz CE, Duran FL, Busatto GF, Gillies DF, Rueckert D. 2007. Multivariate statistical differences of MRI samples of the human brain. J Math Imaging Vis 29:95–106.

Wang J, Wang X, Xia M, Liao X, Evans A, He Y. 2015. GRETNA: a graph theoretical network analysis toolbox for imaging connectomics. Front Hum Neurosci 9:386.

Wang J-H, Zuo X-N, Gohel S, Milham MP, Biswal BB, He Y. 2011. Graph theoretical analysis of functional brain networks: test-retest evaluation on short-and long-term resting-state functional MRI data. PLoS One 6:e21976.

Wang K, Jiang T, Yu C, Tian L, Li J, Liu Y, et al. 2008. Spontaneous activity associated with primary visual cortex: a resting-state FMRI study. Cereb Cortex 18:697–704.

Weissenbacher A, Kasess C, Gerstl F, Lanzenberger R, Moser E, Windischberger C. 2009. Correlations and anticorrelations in resting-state functional connectivity MRI: a quantitative comparison of preprocessing strategies. Neuroimage 47:1408–1416.

Wu L, Eichele T, Calhoun VD. 2010. Reactivity of hemodynamic responses and functional connectivity to different states of alpha synchrony: a concurrent EEG-fMRI study. Neuroimage 52:1252–1260.

Xu P, Huang R, Wang J, Van Dam NT, Xie T, Dong Z, et al. 2014. Different topological organization of human brain functional networks with eyes open versus eyes closed. Neuroimage 90:246–255.

Yan C, Cheung B, Kelly C, Colcombe S, Craddock RC, Di Martino A, et al. 2013. A comprehensive assessment of regional variation in the impact of head micromovements on functional connectomics. Neuroimage 76:183–201.

Yan C, Liu D, He Y, Zou Q, Zhu C, Zuo X, et al. 2009. Spontaneous brain activity in the default mode network is sensitive to different resting-state conditions with limited cognitive load. PLoS One 4:e5743.

Yang H, Long X-Y, Yang Y, Yan H, Zhu C-Z, Zhou X-P, et al. 2007. Amplitude of low frequency fluctuation within visual areas revealed by resting-state functional MRI. Neuroimage 36:144–152.

Yu-Feng Z, Yong H, Chao-Zhe Z, Qing-Jiu C, Man-Qiu S, Meng L, et al. 2007. Altered baseline brain activity in children with ADHD revealed by resting-state functional MRI. Brain Dev 29:83–91.

Zhang D, Liang B, Wu X, Wang Z, Xu P, Chang S, et al. 2015. Directionality of large-scale resting-state brain networks during eyes open and eyes closed conditions. Front Hum Neurosci 9:81.

Zou Q, Long X, Zuo X, Yan C, Zhu C, Yang Y, et al. 2009. Functional connectivity between the thalamus and visual cortex under eyes closed and eyes open conditions: a resting-state fMRI study. Hum Brain Mapp 30:3066–3078.

Zou Q, Miao X, Liu D, Wang DJ, Zhuo Y, Gao J-H. 2015. Reliability comparison of spontaneous brain activities between BOLD and CBF contrasts in eyes-open and eyes-closed resting states. Neuroimage 121:91–105.

Zubek JP. 1969. *Sensory Deprivation: Fifteen Years of Research*. London: Ardent Media.

Zuo XN, Ehmke R, Mennes M, Imperati D, Castellanos FX, Sporns O, et al. 2012. Network centrality in the human functional connectome. Cereb Cortex 22:1862–1875.

Zuo X-N, Kelly C, Adelstein JS, Klein DF, Castellanos FX, Milham MP. 2010. Reliable intrinsic connectivity networks: test–retest evaluation using ICA and dual regression approach. Neuroimage 49:2163–2177.

Address correspondence to:
Ming Liu
Center for the Study of Applied Psychology
Key Laboratory of Mental Health and Cognitive Science of
Guangdong Province
School of Psychology
South China Normal University
Guangzhou 510631
China

E-mail: lium@scnu.edu.cn